Observation of antiphase boundaries in Sr_2FeMoO_6

J. Lindén
Department of Physics, Åbo Akademi, FIN-20500 Turku, Finland

M. Karppinen,* T. Shimada, Y. Yasukawa, and H. Yamauchi
Materials and Structures Laboratory, Tokyo Institute of Technology, Yokohama 226-8503, Japan

(Received 10 September 2002; revised manuscript received 25 June 2003; published 11 November 2003)

A high-purity Sr_2FeMoO_6 sample was synthesized. According to Rietveld analysis of x-ray diffraction (XRD) data the occupancy of Fe at its regular *B* site was 95.6% with the rest occupying the Mo site, i.e., the antisite of Fe. Despite this, according to ^{57}Fe Mössbauer spectra 22% of the Fe atoms resided in a trivalent state having an extremely low internal field of $\sim$2.8 T even at 5 K, whereas a typical 46-T field was seen for the main component, which is known to arise from mixed-valence $Fe^{II/III}$. Since the low-field Fe^{III} species were totally invisible to probing by XRD measurements, it is suggested that they are atoms located on antiphase boundaries (APB's). Magnetization measurements revealed a slightly lowered saturation magnetization (M_s) for the sample exhibiting the highest concentration of APB's, as compared to samples with low concentration of APB atoms. The two-Fe-atom-thick APB layer consists of Fe atoms antiferromagnetically coupled to each other. The spins of the APB layer atoms turned perpendicularly to an applied magnetic field, as observed by Mössbauer spectroscopy.

DOI: 10.1103/PhysRevB.68.174415 PACS number(s): 76.80.+y, 75.47.−m, 75.60.Ch

I. INTRODUCTION

Within the family of *B*-site ordered double perovskites ($A_2BB'O_6$) Sr_2FeMoO_6 has attracted a great deal of interest, due to the half-metallic properties and tunneling-type magnetoresistance (TMR) of the phase.[1] Several schemes for enhancing and/or modifying the magnitude of the magnetoresistance effect have been tested. The influence of Fe/Mo disorder (concentration of Fe at its antisite and vice versa) on the TMR ratio was recently demonstrated.[2–4] Cation substitutions at both *A* and *B* sites were also performed and their effects on the TMR properties are rather well documented.[5–8] Various grain and domain-boundary and impurity-phase effects have been studied.[9,10] These are generally difficult to verify, as most of the experimental techniques used mainly detect bulk properties. The presence of antiphase boundaries (APB's) between regions where the ideal alternating stacking of Fe and Mo atoms starts from the opposite cations has been postulated.[11] Crystallographically the bulk materials on either sides of the APB's are identical, but at the boundary itself Fe-O-Fe bonds are thought to exist due to the phase shift of π in real space over half a lattice constant (Fig. 1). Trials to observe APB in Sr_2FeMoO_6 using ^{57}Fe Mössbauer spectroscopy have thus far been unsuccessful.[12] However, in a previous work presence of APB's was seen in high-resolution electron microscopy images.[13] The influence of APB's in thin films of Fe_3O_4 was recently studied from the magnetoresistance point of view.[14] It was also shown that due to the strong antiferromagnetic (AFM) coupling between the APB atoms the spins will acquire a perpendicular orientation with respect to the bulk magnetization upon subjecting the sample to an external field, Fig. 1.

In this paper we will present evidence for the presence of Fe atoms located on APB's in Sr_2FeMoO_6, as seen using ^{57}Fe Mössbauer spectroscopy. As the method acts as a local probe it is well suited for distinguishing the Fe atoms that are within the APB's from those which are not.

II. EXPERIMENTAL DETAILS

The samples used in the present work were prepared by means of an oxygen-getter-controlled low-O_2-pressure encapsulation technique as developed earlier.[15] In brief, stoichiometric quantities of $SrCO_3$, Fe_2O_3, and MoO_3 powders were mixed and calcined in air at 900 °C for 15 h. The calcined powder mixture was pelletized and encapsulated in an evacuated fused-quartz ampoule containing Fe grains acting as a getter for excess oxygen. The ampoule was then fired at 1150 °C for a period of 50 h and quenched to room temperature by putting the hot ampoule on a thick Cu plate. The thus obtained material was denoted sample 1. Additional samples were synthesized under the same conditions, but with a shorter sintering time (sample 2) or by furnace cooling it after the 50-h sintering (sample 3). The phase purity, crystal symmetry, lattice parameters, and degree of *B*-site order were investigated by x-ray diffraction [XRD, MAC Science: M18XHF[22]. Rietveld analysis using the software RIETAN was done on the XRD data. Magnetization measurements under applied fields of 0–5 T were performed at 5 K and 300 K

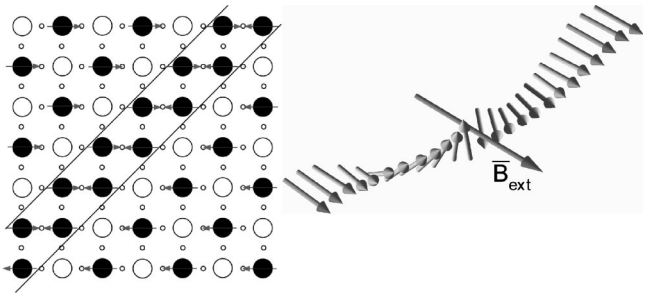

FIG. 1. Schematic illustration of the antiphase boundary. Solid and open circles denote Fe and Mo atoms, respectively. The oxygen atoms are indicated using small circles. For clarity only Fe spins are drawn. The expected Fe spin alignment assuming a domain boundary at the APB's is also shown to the left, Ref. 14.

using a dc superconducting quantum interference device (SQUID) magnetometer (Quantum Design: MPMS-XL).

A Mössbauer absorber was made by spreading the powder (sample 1), mixed with an epoxy resin, on an Al foil. The absorber thickness was ~ 20 mg/cm^2. Spectra were recorded in a transmission geometry using the maximum Doppler velocity of 11.15 mm/s. The absorber temperature was set at 77 K and at 5 K. At 77 K magnetic fields of $B_{\mathrm{ext}}=0$ T, 0.01 T, 0.20 T, 0.40 T, and 0.80 T were applied using permanent Nd-Fe-B magnets. In the two latter cases the direction of the magnetic field was perpendicular to the direction of the γ beam, whereas for 0.01-T and 0.20-T measurements it was parallel. Here 300-K Mössbauer measurements at 0 T and 5 T were also performed using a Mössbauer spectrometer equipped with an superconducting magnet at the Department of Geology at Uppsala University. A Cyclotron Co. ^{57}Co:Rh (25mCi, Jan. 2002) source was used in the 77-K measurements. The full Hamiltonian of combined electric and magnetic interactions was used to fit the spectra, with the total magnetic field experienced by the Fe nucleus (B), the chemical isomer shift relative to α-Fe at 300 K (δ), the quadrupole coupling constant (eQV_{zz}), the resonance line widths (Γ), and the relative intensities of the components (I) as fit parameters. The following conditions and constraints were applied: (i) For each component a certain variation in the parameter B was allowed in order to simulate the fact that the internal fields have a certain spread. A Gaussian distribution was assumed and its width (ΔB) was also introduced as a fit parameter. (ii) The θ angle between the wave vector of the γ quanta and the direction of B was fitted. This angle depends on how the applied field B_{ext} manages to align the magnetization of the domains. Also the angle β, which specifies the direction of the magnetic field with respect to V_{zz}, was fitted for the main components. The asymmetry parameter η and the additional angles α and ϕ were fixed at zero. (iii) All spectral components were constrained to have equal line widths Γ.

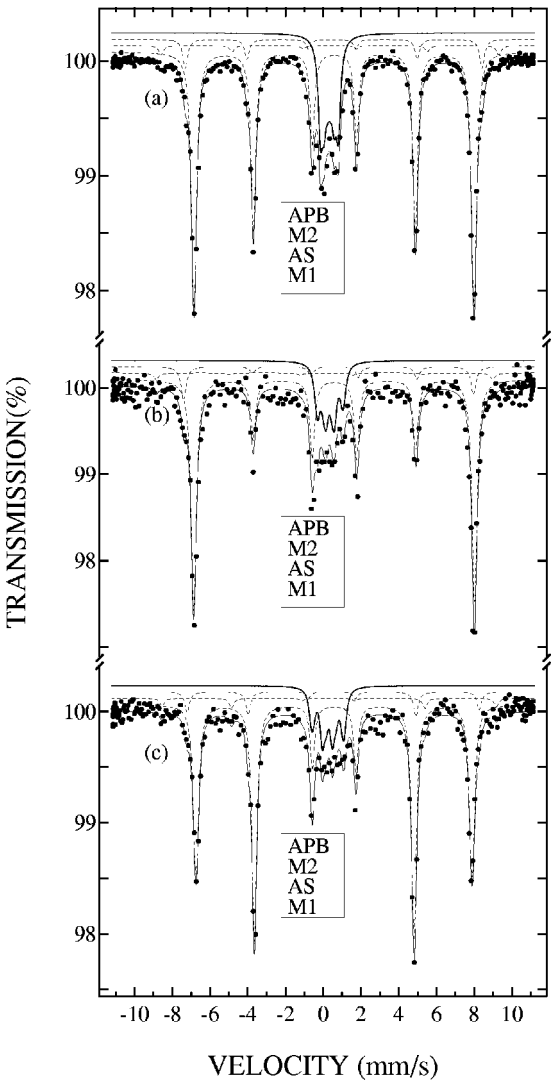

FIG. 2. Mössbauer spectra of the Sr_2FeMoO_6 sample 1 measured at 77 K in applied fields of (a) 0 T, (b) 0.20 T, and (c) 0.80 T. The components used in the fittings are displayed above the data. The labeling of the components is found in the legends, in the same order as the components.

III. RESULTS AND DISCUSSION

According to x-ray diffraction data all samples were phase pure. From a Rietveld refinement of sample 1 in space group $I4/m$, the regular Fe site was found to be 95.6(5)% occupied by Fe. The saturation magnetic moment (M_s) at 5 K was $3.70(2)\mu_{\mathrm{B}}$. For sample 2, $M_s=3.91(2)\mu_{\mathrm{B}}$ was obtained. In Fig. 2 Mössbauer spectra obtained for sample 1 at 77 K in applied fields of 0 T, 0.20 T, and 0.80 T are shown. The spectra were fitted using four spectral components, and the hyperfine parameters obtained from the fittings are presented in Table I. The 5-K data are not presented, as they were similar to the 0-T 77-K data. The fitted value for θ_{expt} illustrates well the increase in degree of domain alignment in the parallel ($\|, \theta_{\mathrm{expt}} \rightarrow 0°$) and perpendicular geometries ($\perp, \theta_{\mathrm{expt}} \rightarrow 90°$) upon increasing B_{ext}. The spectra were dominated by a component (denoted $M1$) with an internal field of ~ 46 T and an isomer shift of ~ 0.7 mm/s, which in accordance with previous results, was assigned to a mixed-valence state of $Fe^{II/III}$ (Ref. 16). This assignment is based on the lower-than-expected internal field value, as well as the isomer shift value, which is halfway between that of high-spin Fe^{III} and Fe^{II}. Furthermore, there is a strong mixing of the itinerant d electron from the Mo^{V} and the minority spin t_{2g} band of Fe^{III} (Ref. 1), which causes the decrease in the valence state of Fe from III toward II/III. The scattering of the β values for $M1$ in Table I is a result of the very small eQV_{zz} value. Antisite Fe has earlier been shown to give rise to a Mössbauer component with a large internal field,[16] and such a component is indeed present in the present Mössbauer data as well (denoted AS). It covered the expected $\sim 3\%$ intensity in accordance with the Rietveld results. Component AS is well resolved only in the 77-K spectra measured under zero applied field, due to the better statistics. An additional component ($M2$) has a large internal field (~ 47 T at 77 K) and an isomer shift value of ~ 0.6 mm/s, i.e., it seems to be somewhere between typical Fe^{III} and $Fe^{II/III}$. Following Ref.

TABLE I. Hyperfine parameters obtained from the fit of the spectra of the Sr_2FeMoO_6 sample 1 at 77 K and 300 K. The latter data are in the last two columns. Cases where the lower limit has been reached are indicated with an L.

Comp.	Param.	0 T	0.01 T$\parallel$	0.20 T$\parallel$	0.40 T$\perp$	0.80 T$\perp$	0 T	5.0 T$\parallel$
	θ_{expt}	54.74° [a]	52(1)°	36(1)°	73(1)°	79(2)°	54.74 [a]	9(2)°
$M1/M1'$	δ (mm/s)	0.702(1)	0.693(4)	0.708(7)	0.700(3)	0.698(3)	0.51/0.51	0.53/0.51
	B (T)	45.84(1)	45.97(3)	45.98(4)	45.53(2)	45.18(2)	34.2/30.7	30/27
	I (%)	69(1)	71(3)	69(3)	71(2)	73(2)	50/23	51/23
	eQV_{zz}(mm/s)	−0.42(5)	−0.0(2)	−0.4(3)	−0.4(2)	−0.5(2)	0.0/−0.3	−0.6/−1.4
	β (deg)	−50(20)	164(8)	51(8)	53(5)	−53(2)	−103/94	52/123
APB	δ (mm/s)	0.44(1)	0.45(2)	0.45(5)	0.34(3)	0.40(4)	0.30(3)	0.30(4)
	B (T)	2.86(6)	2.95(2)	3.6(2)	3.9(3)	4.33(4)	2.74(3)	5.70(4)
	I (%)	21(1)	22(2)	20(1)	20(2)	17(3)	19(2)	18(3)
	eQV_{zz}(mm/s)	−0.20(3)	−0.3(1)	0.8(3)	−0.9(1)	−1.0(2)	−0.3(2)	−0.6(3)
	β (deg)	−63(20)	−50(5)	−42(20)	−45(7)	−45(9)	−55(5)	−49(5)
	θ_{APB} (deg)	62(6)	61(10)	80(10)	83(5)	78(3)	70(4)	60(4)
AS	δ (mm/s)	0.47(4)	0.39(6)	0.24(9)	0.37(7)	0.42(5)	0.50(6)	0.7(1)
	B (T)	55.3(3)	54.8(5)	55.1(4)	55.2(8)	54.7(4)	40.6(5)	46.0(4)
	I (%)	2.4(3)	4(1)	2(L)	2.9(9)	2.9(8)	2(1)	2(L)
	eQV_{zz}(mm/s)	0.6(1)	2.2(2)	0.6(3)	−0.5(3)	0.5(2)	0.1(2)	2.0(4)
	β (deg)	−53(6)	−60(10)	−76(30)	28(5)	−46(7)	−92(7)	−92(6)
$M2$	δ (mm/s)	0.63(1)	0.54(5)	0.57(4)	0.44(3)	0.62(3)	0.58(4)	0.48(5)
	B (T)	48.4(2)	47.8(4)	47.1(5)	48.2(3)	47.6(3)	27.2(4)	23.6(3)
	I (%)	7.3(6)	4(L)	9(2)	7(1)	7(1)	6(1)	6(1)
	eQV_{zz}(mm/s)	−1.6(4)	−0.6(1)	−2.0(9)	−1.7(9)	−1.6(7)	0.2(3)	1.1(4)
	β (deg)	59(1)	180(6)	42(6)	48(8)	58(2)	−3(8)	44(5)

[a]Fixed at the so-called magic angle for a randomly oriented sample.

12 it may be assigned to Fe at sites adjacent to an antisite Fe atom.

The most striking feature of the zero-field spectra (Fig. 2) is the low-field component (denoted APB) located around zero velocity. It covered 22% of the spectral intensity at 0 T and appeared to be Fe^{III}, due to its isomer shift of ~0.40 mm/s, indicating that it did not participate in forming any mixing valence with Mo. Also, for other A_2FeMoO_6 samples having Ca, Ba, or Sr at the A site, we recently observed the APB component in the Mössbauer spectra.[17] In 0-T and 77-K measurements of samples 2 and 3 the presence of APB's was found, but its portion was only ~8%. Upon increasing the applied field the APB component of sample 1 changed appearance drastically. In our first attempts the APB subspectrum in nonzero applied field could only be fitted using two components. Then a separate angle θ_{APB}, between the γ beam and the internal field of the APB Fe atoms, was introduced and fitting using only one APB component became possible. This is due to the fact that when θ_{expt} approaches 0°, lines 2 and 5 in the Mössbauer sextet are weakened or missing. However, for this case $\theta_{APB} \rightarrow 90°$, as explained below, and lines 2 and 5 are instead enhanced for the APB sextet. When fitting the spectra using only one global θ_{expt} parameter the other fictive APB component simply accounted for the missing lines 2 and 5.

In order to further study the dynamics of the APB component 300-K spectra were recorded in external fields of 0.0 and 5.0 T, Fig. 3. These spectra were also fitted using the spectral components $M1$, $M2$, AS, and APB. However, $M1$ is split into two components (denoted $M1$ and $M1'$ in Fig. 3) at 300 K (Ref. 16) and the $M2$ component has a lower field than $M1$, but otherwise the spectra are rather similar. In overall the internal-field values are decreased due to the increase in temperature. The relative intensity and internal field of the APB component are roughly the same at 5, 77, and 300 K. The results are included in Table I.

Generally it was observed that θ_{APB} followed a different trend than θ_{expt}, Fig. 4. The behavior can be explained using Fig. 1. When the γ-ray beam is parallel to the external field, the bulk magnetization of the (partially) magnetized sample is also parallel to the direction of the beam (hence $\theta_{expt} \rightarrow 0°$). In this case obviously $\theta_{APB} \rightarrow 90°$. Upon increasing the field strength (in our case to 5 T) the sample magnetizes completely and θ_{APB} should in principle be 90°, but instead a decrease is observed. This is due to the fact that the total field B observed in the Mössbauer spectrum is the vector sum of the internal field $\vec{B}_{int}$ and the applied field $\vec{B}_{ext}$ (plus the field due to the bulk magnetization). When $\vec{B}_{ext}$ is increased the total field $\vec{B}$ will be increasingly parallel to the applied field, explaining the decrease. Two data points were also recorded in the perpendicular geometry in a modest field, where θ_{expt} and θ_{APB} values slightly less than 90° are expected. However, for strong external field strengths θ_{APB} would eventually converge toward 90°, for similar reasons as presented for the parallel geometry. The total APB field as

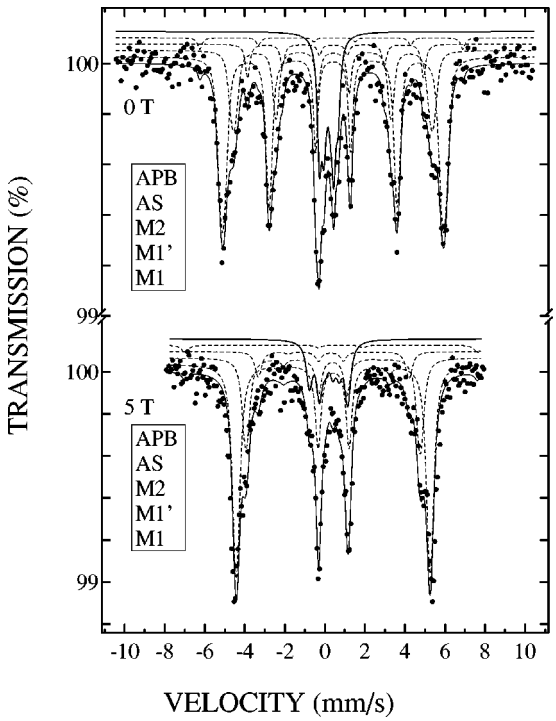

FIG. 3. Mössbauer spectra of the Sr_2FeMoO_6 sample 1 measured at 300 K in applied fields of (a) 0 T, (b) 5.0 T, and (c) 0.80 T. The components used in the fittings are displayed above the data. The labeling of the components is found in the legends, in the same order as the components.

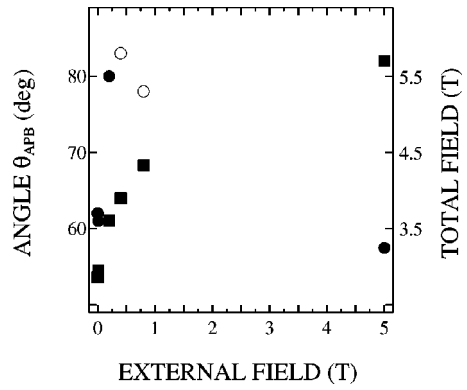

FIG. 4. Dependence of the angle θ_{APB} (circles) and the total field (squares) on the external field strength, as analyzed from the Mössbauer spectra of sample 1. Solid and open circles represent data obtained in the parallel ($\theta_{expt} \rightarrow 0°$) and perpendicular ($\theta_{expt} \rightarrow 90°$) geometries, respectively.

a function of B_{ext} is also plotted in Fig. 4. The very strong increase for low external fields is due to the domain alignment, which occurs even in weak fields and also acts directly on the APB atoms.

At this point it is illustrative to review the alternative explanation of the APB component—namely, an impurity phase. The strong overall intensity of the APB component ruled out the possibility of an impurity phase, as XRD and magnetization observations indicated a high phase purity. From a chemical point of view any other Fe atoms than those in the bulk would be in a valence state of II, due to the highly reductive synthesis conditions. However, Fe^{II} impurities would appear with an isomer shift of more than 1.0 mm/s, in further support of the origin of the APB component. Additional information is obtained from the behavior of the total field. The direction of the total field of a paramagnetic impurity would simply be that of the applied field, and its value would be a sum of the bulk magnetization and the external field. The direction of the total field for a ferromagnetic impurity, which is very unlikely to occur, considering that the APB component originates from a trivalent oxide, would also follow the direction specified by θ_{expt}. Furthermore, as the Fermi-contact interaction that mediates the internal magnetic field originating from the Fe *d* electrons has opposite direction as the bulk magnetization,[20] a decrease would initially be seen in the total field upon increasing B_{ext}, ruling out this possibility. Note that the decrease in the field values of $M1$ and $M2$ illustrates this decrease of total field for ferromagnetic components. For component AS the situation is the opposite, as the total field increases due to its antiferromagnetic coupling to the bulk magnetization.[12] The third possibility, i.e., an (isolated) antiferromagnetic impurity phase is also out ruled. In modest fields ($B_{ext} < 1.0$ T) antiferromagnetic impurities would only exhibit line broadening, as the external field randomly adds or subtracts to the total field. On the average the total field would remain roughly the same and θ_{APB} at the random angle 54.74°.

The unique behavior of the APB component in an external magnetic field confirms that the two adjacent Fe atoms within the APB's are antiferromagnetically coupled to each other and ferromagnetically coupled to the bulk. Our samples were also investigated by means of state-of-the-art electron microscopy techniques and presence of antiphase boundaries was clearly seen.[18]

Using the APB component intensity we can now calculate the average diameter of a domain (presumed spherical) that is surrounded by an APB (Ref. 12): $D = 12a/I_{APB}$, where $a \approx 7.90$ Å is the lattice parameter of the (pseudo)cubic unit cell and the numerical factor 12 ($=2\times3\times2$) originates from the facts that there are two Fe atoms within the width of the APB, the surface to volume ratio of a sphere (which contributes with a factor 3), and that D is twice the radius. Using the value $I_{APB} = 0.22$ we get $D \approx 430$ Å, which is of the same order of magnitude as, e.g., the one reported for the domain size in thin films of Fe_3O_4 (Ref. 19).

According to the predictions APB atoms should experience a strong AFM coupling, due to the almost ideal Fe-O-Fe superexchange bond.[21] In thin films of Fe_3O_4 that exhibited APB's, the saturation fields were accordingly found to be large as strong applied fields were required to force the AFM Fe species to align with the bulk magnetization.[19] The same is apparently true for the present case as well, as 5 T is not enough to break the bonds of the APB Fe atoms and force them to join the bulk magnetization. The extremely low internal field value of the APB atoms is unexpected. Possibly there is a strong competition between the AF superexchange of the Fe-O-Fe bond in the APB and ferromagnetic double-exchange interactions. This is a point which needs to be clarified in future works.

The APB component has not been reported earlier for Mössbauer spectra of Sr_2FeMoO_6 and related phases. However, small amounts of a possible APB component can be seen in some published data, but it has been left unfitted; cf., e.g., the 77-K spectra of Ba_2FeMoO_6 in Ref. 22. In principle the APB's could also be based on Mo atoms, but these would not be visible in the Mössbauer data. Chemically a Mo-based APB would be rather instable, due to the high Mo valence.

IV. CONCLUSIONS

We obtained evidence for Fe atoms located on antiphase boundaries based on Mössbauer spectra for a high-purity Sr_2FeMoO_6 sample. Using the Mössbauer data obtained under an applied field we showed that the spins of the APB atoms orient perpendicularly to the bulk magnetization, confirming the antiferromagnetic coupling between the Fe atoms within the antiphase boundary. The internal field of the APB Fe atoms was unusually small, only ~ 2.8 T at 77 K.

Note added in proof. In a very recent Mössbauer measurement of a sol-gel synthesized Sr_2FeMoO_6 sample we observed a rather intense low-field component similar to component APB. Due to the small particle size of the powder sample, presence of anti-phase boundaries was not expected. In the Mössbauer spectrum measured in an external field this component had almost completely merged with $M1$, proving that it orginated from superparamagnetism and was not related to antiphase boundaries, despite the similarity of the 0-T Mössbauer data.

ACKNOWLEDGMENTS

Yassir Abdu is acknowledged for the 300-K 0- and 5-T measurements. Kim Gustafsson and Nikolai Kaihovirta are acknowledged for their contributions to the 77-K Mössbauer measurements. Tauno Ahlfors is acknowledged for designing the magnets for the 77-K Mössbauer measurements. This work was supported by Grants-in-Aid for Scientific Research (Nos. 15206002 and 15206071) from the Japan Society for the Promotion of Science. Support from the JSPS Research (Grant No. 14006635) is acknowledged by Y.Y. and support from the Scandinavia-Sasakawa Foundation and Magnus Ehrnrooth Foundation is acknowledged by J.L.

*Corresponding author. Electronic address: karppinen@msl.titech.ac.jp

[1] K.-I. Kobayashi, T. Kimura, H. Sawada, K. Terakura, and Y. Tokura, Nature (London) **395**, 677 (1998).
[2] A.S. Ogale, S.B. Ogale, R. Ramesh, and T. Venkatesan, Appl. Phys. Lett. **75**, 537 (1999).
[3] D.D. Sarma, E.V. Sampathkumaran, S. Ray, R. Nagarajan, S. Majumdar, A. Kumar, G. Nalini, and T.N. Guru Row, Solid State Commun. **114**, 465 (2000).
[4] M. García-Hernándezs, J.L. Martínez, M.J. Martínez-Lope, M.T. Casais, and J.A. Alonso, Phys. Rev. Lett. **86**, 2443 (2001).
[5] A. Maignan, B. Raveau, C. Martin, and M. Hervieu, J. Solid State Chem. **144**, 224 (1999).
[6] K.-I. Kobayashi, T. Kimura, Y. Tomioka, H. Sawada, K. Terakura, and Y. Tokura, Phys. Rev. B **59**, 11 159 (1999).
[7] K.-I. Kobayashi, T. Okuda, Y. Tomioka, T. Kimura, and Y. Tokura, J. Magn. Magn. Mater. **218**, 17 (2000).
[8] J. Lindén, T. Yamamoto, J. Nakamura, H. Yamauchi, and M. Karppinen, Phys. Rev. B **66**, 184408 (2002).
[9] H. Han, B.J. Han, J.S. Park, B.W. Lee, S.J. Kim, and C.S. Kim, J. Appl. Phys. **89**, 7687 (2001).
[10] D. Niebieskikwiat, A. Caneiro, R.D. Sánchez, and J. Fontcuberta, Phys. Rev. B **64**, 180406 (2001).
[11] J.B. Goodenough and R.I. Dass, Int. J. Inorg. Mater. **2**, 3 (2000).
[12] J.M. Greneche, M. Venkatesan, R. Suryanarayanan, and J.M.D. Coey, Phys. Rev. B **63**, 174403 (2001).
[13] J. Navarro, Ll. Balcells, F. Sandiumenge, M. Bibes, A. Roig, B. Martínez, and J. Fontcuberta, J. Phys.: Condens. Matter **13**, 8481 (2001).
[14] W. Eerenstein, T.T.M. Palstra, S.S. Saxena, and T. Hibma, Phys. Rev. Lett. **88**, 247204 (2002).
[15] T. Yamamoto, J. Liimatainen, J. Lindén, M. Karppinen, and H. Yamauchi, J. Mater. Chem. **10**, 2342 (2000).
[16] J. Lindén, T. Yamamoto, M. Karppinen, H. Yamauchi, and T. Pietari, Appl. Phys. Lett. **76**, 2925 (2000).
[17] Y. Yasukawa, J. Lindén, T.S. Chan, R.S. Liu, H. Yamauchi, and M. Karppinen (unpublished).
[18] T. Asaka and Y. Matsui (unpublished).
[19] D.T. Margulies, F.T. Parker, M.L. Rudee, F.E. Spada, J.N. Chapman, P.R. Aitchison, and A.E. Berkowitz, Phys. Rev. Lett. **79**, 5162 (1997).
[20] R.W. Grant, in *Mössbauer Spectroscopy*, edited by U. Gonser (Springer, Berlin, 1975), p. 106.
[21] L. Berger, Y. Labaye, and J.M.D. Coey, J. Magn. Magn. Mater. **242–245**, 1221 (2002).
[22] J. Gopalakrishnan, A. Chattopadhyay, S.B. Ogale, T. Venkatesan, R.L. Greene, A.J. Millis, K. Ramesha, B. Hannoyer, and G. Marest, Phys. Rev. B **62**, 9538 (2000).